

Article

The Natural Product Lepidiline A as an *N*-Heterocyclic Carbene Ligand Precursor in Complexes of the Type $[\text{Ir}(\text{cod})(\text{NHC})\text{PPh}_3]\text{X}$: Synthesis, Characterisation, and Application in Hydrogen Isotope Exchange Catalysis

Alison R. Cochrane, Alan R. Kennedy, William J. Kerr , David M. Lindsay , Marc Reid  and Tell Tuttle 

Department of Pure and Applied Chemistry, WestCHEM, University of Strathclyde, Glasgow G1 1XL, Scotland, UK; alison.r.cochrane@gmail.com (A.R.C.); a.r.kennedy@strath.ac.uk (A.R.K.); david.lindsay@strath.ac.uk (D.M.L.); marc.reid.100@strath.ac.uk (M.R.); tell.tuttle@strath.ac.uk (T.T.)

* Correspondence: w.kerr@strath.ac.uk

Received: 20 December 2019; Accepted: 26 January 2020; Published: 1 February 2020



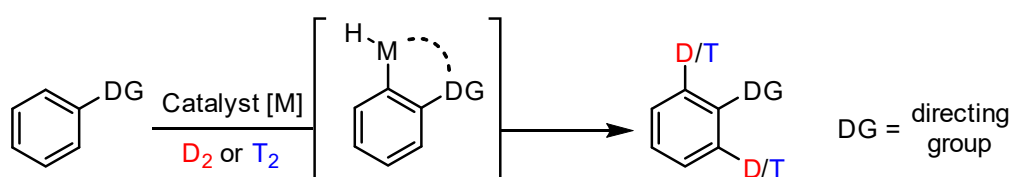
Abstract: A range of iridium(I) complexes of the type $[\text{Ir}(\text{cod})(\text{NHC})\text{PPh}_3]\text{X}$ are reported, where the *N*-heterocyclic carbene (NHC) is derived from the naturally-occurring imidazolium salt, Lepidiline A (1,3-dibenzyl-4,5-dimethylimidazolium chloride). A range of complexes were prepared, with a number of NHC ligands and counter-ions, and various steric and electronic parameters of these complexes were evaluated. The activity of the $[\text{Ir}(\text{cod})(\text{NHC})\text{PPh}_3]\text{X}$ complexes in hydrogen isotope exchange reactions was then studied, and compared to established iridium(I) complexes.

Keywords: iridium; *N*-heterocyclic carbene; hydrogen isotope exchange; deuterium

1. Introduction

Isotopically labelled compounds are of importance in a range of scientific disciplines. In particular, the isotopes of hydrogen, deuterium, and tritium find application in several key areas. Within the physical sciences, deuterated compounds are routinely used in the elucidation of reaction mechanisms [1]. In the life sciences, deuterated and tritiated compounds are used to determine the pharmacokinetic properties of bioactive molecules [2–4]. More recently, active pharmaceutical ingredients themselves have begun to feature deuterium, exploiting the effect of relative C-H/C-D bond strengths to deliver drug molecules with improved metabolic profiles [5,6].

Amongst the synthetic methods available for incorporation of deuterium or tritium into a molecule, hydrogen isotope exchange (HIE) stands out due to its simplicity and generality [7–9]. A particularly powerful variant of this process is directed HIE, whereby a Lewis basic group within the molecule directs a metal catalyst to an adjacent site, and a subsequent C-H activation results in a metalcyclic intermediate which facilitates HIE at this adjacent position (Scheme 1).



Scheme 1. Directed hydrogen isotope exchange.

Iridium(I) complexes are amongst the most effective metal catalysts for directed HIE [10] and, in recent years, we have introduced a suite of highly active Ir(I) catalysts bearing a combination of bulky phosphine and *N*-heterocyclic carbene ligands (Figure 1). These catalysts are compatible with a broad variety of directing groups, enabling HIE on a wide range of substrates [11–18].

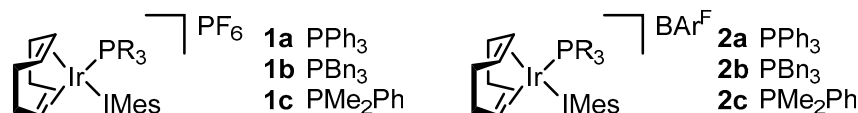


Figure 1. Iridium(I) *N*-heterocyclic carbene (NHC)/phosphine complexes for directed hydrogen isotope exchange.

These benchmark complexes 1–2 feature three distinct phosphine ligands. However, our early studies [11,12], which focused on identifying the most effective catalyst system, evaluated a broader range of phosphines based on their steric and electronic properties. In contrast, although we have optimised the NHC ligand for some specific HIE use cases [19,20], there remains scope for a more systematic study of the steric and electronic parameters of this ligand component. The natural product Lepidiline A **3·HCl** is an imidazolium chloride salt, featuring two *N*-benzyl substituents, and methyl groups at the heterocycle's 4- and 5-positions [21] (Figure 2). We envisaged that this naturally-occurring imidazolium salt could serve as a vehicle to begin to explore the effect of steric and electronic changes in the NHC on the activity of our Ir(I) NHC/phosphine catalysts [22].

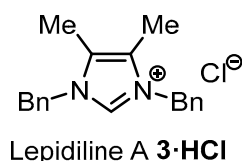


Figure 2. Naturally-occurring imidazolium salt Lepidiline A **3·HCl**.

Herein we report a study of the complexes **1a**, **6a** and **7**, of the type [Ir(cod)(NHC)PPh₃][PF₆] (cod = 1,5-cyclooctadiene), where the NHC ligand is IMes **4**, IBn **5**, or IBn^{Me} **3**, derived from Lepidiline A **3·HCl** (Figure 3). These complexes are then used to explore the effect of steric and electronic variance within the NHC through comparison of (a) *N*-benzyl vs. *N*-mesityl substituents; and (b) 4,5-H₂ vs. 4,5-Me₂ substitution, on the reactivity in HIE processes. The effect of the counter on the activity of the IBn^{Me} complexes is also investigated.

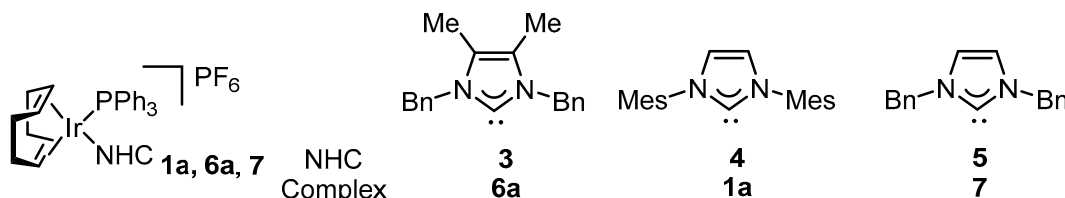


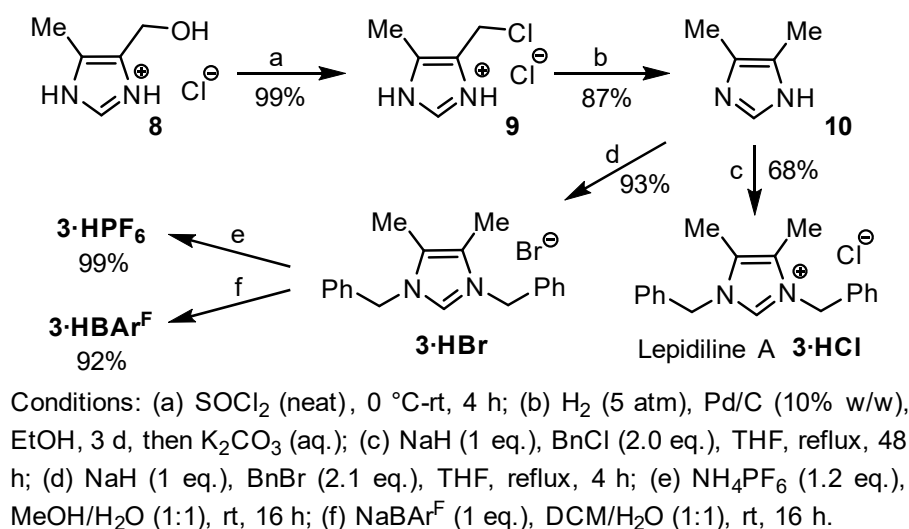
Figure 3. Iridium(I) complexes with varying NHC ligands to probe their steric and electronic influence.

2. Results and Discussion

To initiate our studies, we set out to prepare quantities of the desired [Ir(cod)(NHC)PPh₃][PF₆] complexes **1a**, **6a** and **7**. Complex **1a** was prepared by a modification of previously reported conditions [11,23]. The IBn-containing complex **7** was prepared [23] by using an analogous procedure from the previously reported complex [Ir(cod)(IBn)Cl] [24]. Lastly, the imidazolium chloride salt **3·HCl**, representing the natural product Lepidiline A, was targeted to deliver complex **6a**.

2.1. Synthesis of Lepidiline A

Surprisingly, to our knowledge, no preparation of this naturally-occurring material has yet been reported. Our synthetic route is summarised in Scheme 2. Chlorination of the commercially available hydroxymethyl imidazolium salt **8** in neat thionyl chloride was easily achieved in excellent yield on a multi-gram scale to deliver **9**. Reduction and basification of **9** yielded the free 4,5-dimethylimidazole **10** with good levels of efficiency. Subsequently, double-alkylation of **10** under basic conditions could be achieved using benzyl chloride to give Lepidiline A **3·HCl** with good effectiveness, or with benzyl bromide to give **3·HBr** in excellent yield. Imidazolium bromide **3·HBr** could then undergo salt metathesis to very efficiently afford **3·HPF₆** and **3·HBAr^F**.



Scheme 2. Synthesis of Lepidiline A and counter-ion analogues.

Following the successful preparation of Lepidiline A **3·HCl** and a range of its counterion derivatives, X-ray quality crystals of **3·HCl** were grown and the structure solved to reveal a molecular footprint in direct agreement with the spectroscopic data and the reported natural product structure. The crystal structure was found to be a solvate containing one molecule of water per cation (Figure 4, left). The same cationic motif was found in the X-ray structure of **3·HPF₆**. This latter structure has two crystallographically independent salt units per asymmetric unit (*Z'* = 2). Both cations in this structure adopt *anti* conformations of the benzyl rings with respect to the heteroaromatic ring (Figure 4, right). This is in contrast to the *syn* conformation found for **3·HCl** and in the Ir complexes described below.

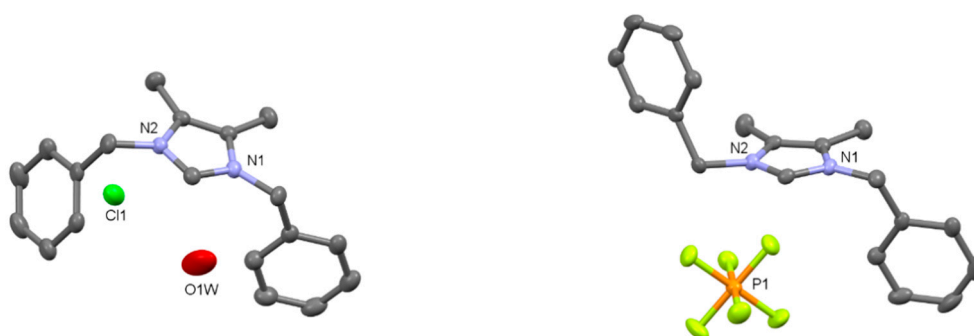
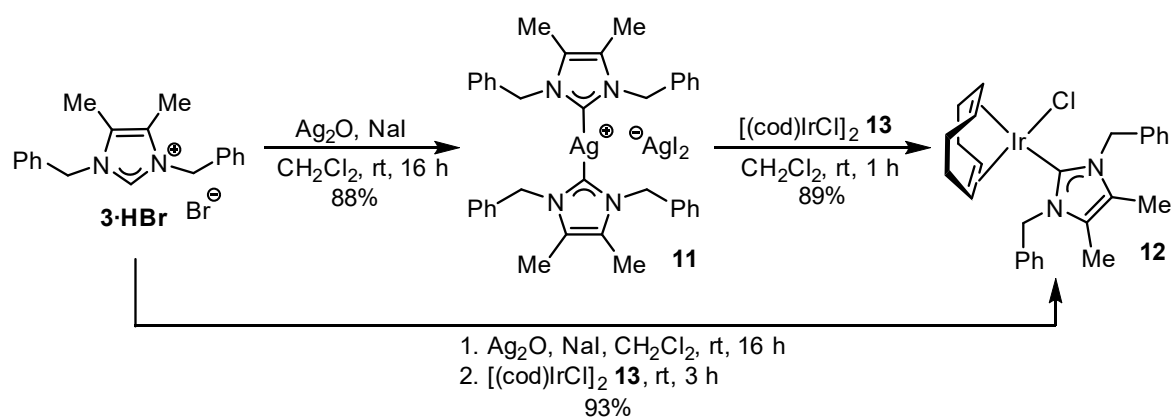


Figure 4. Structures of Lepidiline A (left) and its PF₆ derivative (right) as determined by single crystal diffraction. Atoms are shown as 50% probability ellipsoids. H atoms, disorder in the solvent, and anion of **3·HCl** and the second independent cation-anion pair of **3·HPF₆** have been omitted for clarity.

2.2. Preparation of Iridium Complexes Based on Lepidiline A 3

With a range of imidazolium salt precursors in hand, formation of the corresponding iridium complexes was investigated. Based on work by Wang and Lin [25], and Liu et al. [26], the [(cod)Ir(NHC)Cl] complexes can be prepared via a transmetallation procedure from the corresponding silver bis-carbene complex. Employing the bromide salt **3·HBr**, mixing with silver(I) oxide and sodium iodide in dichloromethane gave silver complex **11** in high yield (Scheme 3). This intermediate could be taken forward into a transmetallation procedure with [(cod)IrCl]₂ **13** to provide the desired chloro-carbene complex **12** in excellent yield following a short reaction time. Alternatively, it was also found that isolation of **11** could be circumvented via direct addition of [(cod)IrCl]₂ **13** following in situ formation of the silver complex **11**, delivering **12** in a further improved overall yield. With this high-yielding method in place, X-ray quality crystals of **12** were grown, confirming the proposed structure (Figure 5).



Scheme 3. Preparation of iridium complex **12**.

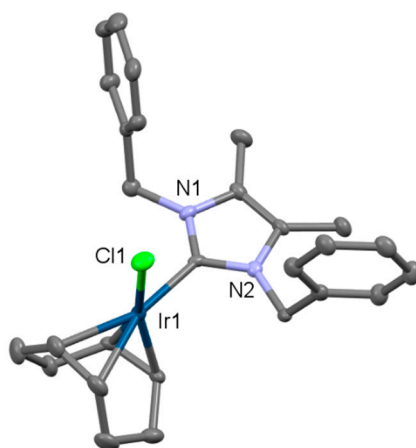


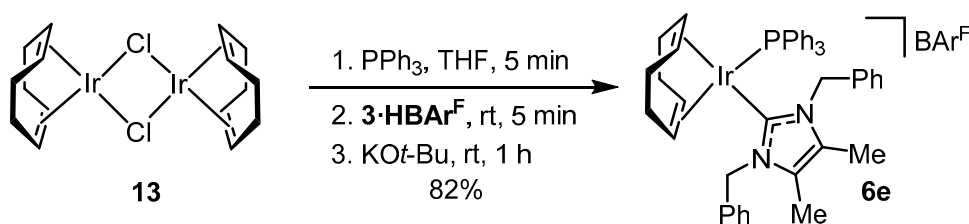
Figure 5. Molecular structure of **12** as determined by single crystal diffraction. Atoms are shown as 50% probability ellipsoids. H atoms and disorder in the orientation of one phenyl ring have been omitted for clarity.

With quantities of the NHC chloride complex **12** secured, treatment with triphenylphosphine, followed by silver hexafluorophosphate, delivered target NHC-phosphine complex **6a** in a good 75% yield (Table 1, entry 1). In order to probe the effects of varying the counter-ion in these novel complexes, derivatives **6b–6d** were also prepared in an analogous manner and with excellent isolated yields (Table 1, entries 2–4).

Table 1. Preparation of [(cod)Ir(IBn^{Me})PPh₃]₂X complexes **6a–6d**.

Entry	Complex	X	Yield
1	6a	PF ₆	75
2	6b	BF ₄	87
3	6c	SbF ₆	81
4	6d	OTf	88

We have previously shown that iridium NHC/phosphine complexes bearing a BAR^F (tetrakis [3,5-bis(trifluoromethyl)phenyl]borate) counter-ion have a broader solvent applicability than the corresponding PF₆ complexes [13]. Based on this, BAR^F-containing complex **6e** was prepared in a one-pot procedure from [(cod)IrCl]₂ **13** in a good 82% yield (Scheme 4). Complexes **6a–6e** were all characterized by X-ray crystallography [23].

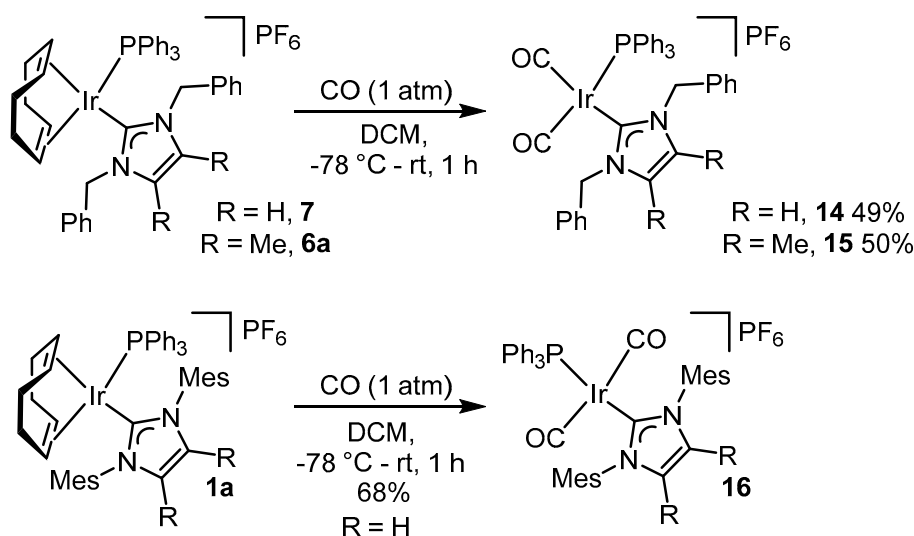
**Scheme 4.** One-pot synthesis of BAR^F counter-ion catalyst **6e**.

2.3. Steric and Electronic Characterisation of the Iridium NHC/Phosphine Complexes

Having successfully prepared a range of Ir complexes containing the Lepidiline A-derived NHC **3**, attention now turned to evaluating this novel ligand sphere versus the alternative ligand sets in PPh₃/IMes complex **1a** and PPh₃/IBn complex **7**. The electronic properties of ligands in a specific complex are often characterised by carbonylation of the complex, whereby the ν_{CO} stretching frequency reports on the electron-donating nature of the other ligands on the metal [27]. Recent work on Ir(I) dicarbonyl complexes has revealed that the configuration of the carbonyl ligands, though preferentially *cis*, is dictated by the ligand size, with larger combinations driving a *trans* dicarbonyl arrangement [28]. This structural fluidity limits the use of electronic parameters derived from such complexes [28]. However, the synthesis and X-ray characterisation of the carbonylated analogues of our NHC/phosphine complexes could instead be used to indicate a steric threshold—the ligand size at which Ir(I) carbonyl complexes switch from a *cis*- to a *trans*-configuration, and this could be correlated with the well-known steric parameter, percentage buried volume, %V_{bur}, [29] of the ligands.

Accordingly, we investigated the carbonylation of complexes **1a**, **6a**, and **7** (Scheme 5). Direct exposure of complexes **6a** and **7** to an atmosphere of CO resulted in complexes **14** and **15**, where both the NHC/phosphine pair and the two CO ligands are each *cis*-orientated, as shown by the X-ray crystal structures [23]. The combined ligand %V_{bur} values (Σ(%V_{bur})) were similar for both complexes, as determined by density functional theory (DFT) calculations (Table 2) [23]. As perhaps expected, the enhanced bulk of the NHC ligand in **1a** resulted in a complex, **16**, with a *trans*-arrangement of the NHC/P pair and of the two CO ligands, indicating the size and geometry of this complex to be quite distinct from the IBn and IBn^{Me} analogues **14** and **15**. Based on these parameters, there is little

steric difference evident on moving from the IBn to the IBn^{Me} ligand, with the latter appearing to be a very slightly bulkier system, based on the %V_{bur} values.



Scheme 5. Preparation of iridium carbonyl complexes **14–16**.

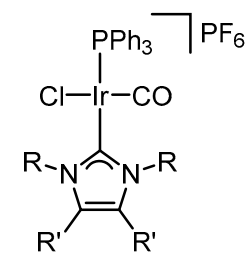
Table 2. Properties of Ir-carbonyl complexes **14–16**.

Entry	Complex	N-Substituent	R	Yield	%V _{bur} (PPh ₃) ²	%V _{bur} (NHC) ²	Σ (%V _{bur})	θ (°) ¹
1	14	Bn	H	49%	26.9	28.9	55.8	93.2
2	15	Bn	Me	50%	27.0	29.2	56.2	89.4 ³ 92.6 ³
3	16	Mes	H	68%	27.9	32.6	60.5	160.0

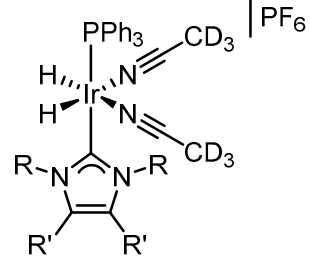
¹ θ represents the angle OC-Ir-CO. ² Representative %V_{bur} values are calculated from DFT-optimized [(NHC)(PPh₃)₂(Ir(H)₂(DCM)₂)⁺ complex cations. Full details are presented in the SI. ³ Carbonyl complex **15** crystallized with two different conformations.

Although these dicarbonyl complexes permitted only a steric, and not electronic, evaluation, literature examples of Ir(I) chloro-carbonyl complexes have demonstrated that the combined influence of various ligand partnerships on the metal's π-donating ability can be measured via IR spectroscopy, based on the carbonyl stretching frequency, ν_{CO} [26,30]. Furthermore, the effect of the ligands on the σ-donating nature of the complex can be measured by ¹H nuclear magnetic resonance (NMR) spectroscopic evaluation of the corresponding dihydride complexes [31]. The electronic characteristics of the IMes, IBn, and IBn^{Me} ligands in our complexes were thus explored by preparing the chloro-carbonyl complexes, **17–19** (Table 3). Additionally, from the NHC/PPh₃ complexes, in situ generation of the dihydride complexes **20–22**, in CD₃CN [23], provided insight into the σ-donating properties (Table 3). Based on both electronic parameters, the IBn^{Me}/PPh₃ combination was found to be slightly more electron-rich than IBn/PPh₃, and more significantly less electron-rich than IMes/PPh₃.

Table 3. Electronic properties of Ir Cl/CO and dihydride complexes.



Cl/CO complex



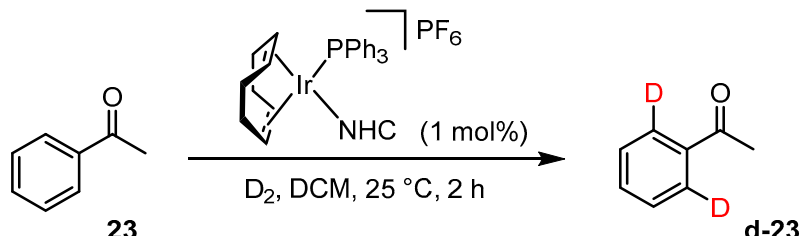
Dihydride complex

Entry	R	R'	Cl/CO Complex	$\nu(\text{CO})_{\text{DCM}}$	Dihydride Complex	δ_{H}
1	Bn	H	17	1950 cm^{-1}	20	−21.35 ppm
2	Bn	Me	18	1948 cm^{-1}	21	−21.40 ppm
3	Mes	H	19	1942 cm^{-1}	22	−21.58 ppm

2.4. Evaluation of Iridium Complex Catalytic Activity in HIE

We next chose to focus on the relationship between the IBn/PPh₃ and IBn^{Me}/PPh₃ complex pair in terms of catalyst activity in HIE reactions. The two precatalysts **6a** and **7** were compared via kinetic analysis of the simple reference labelling reaction with acetophenone **23** (Table 4). Catalyst **6a**, derived from Lepidiline A, was clearly faster reacting, displaying a pseudo first order rate constant, $k_{\text{obs}}(\mathbf{6a}) = 0.0224 \text{ s}^{-1}$, versus $k_{\text{obs}}(\mathbf{7}) = 0.0145 \text{ s}^{-1}$ for IBn/PPh₃ catalyst **7** [23].

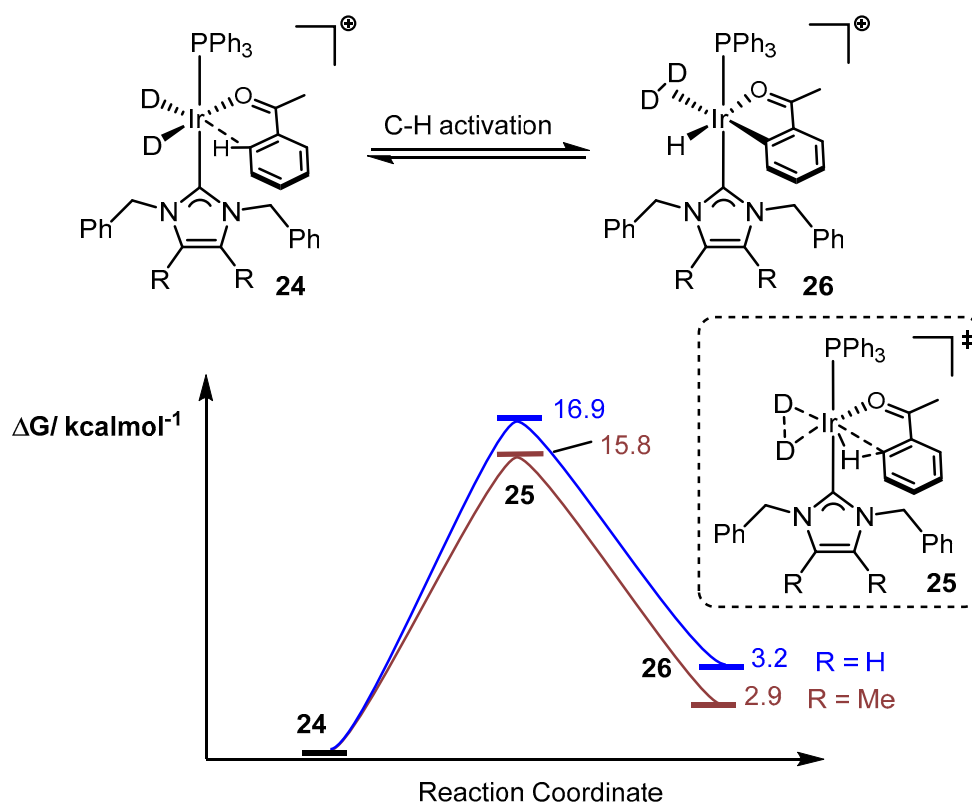
Table 4. Evaluation of complexes **6a** and **7** in a benchmark HIE reaction.



23 **d-23**

Entry	Complex	NHC	k_{obs}
1	6a	IBn ^{Me}	0.0224 s^{-1}
2	7	IBn	0.0145 s^{-1}

This result was supported by DFT modelling of the turnover-limiting [12] C–H activation step (**24**→**26**, Scheme 6). Based on our electronic characterization of these complexes, the greater reactivity of catalyst **6a** over **7** can be rationalised on the basis of an increased π -donating ability of the Ir centre, and not on any appreciable steric difference between the two catalysts **6a** and **7**.



Scheme 6. Computational evaluation of the C-H activation process with catalyst **6a** vs. **7**.

The variation in reactivity between the IBn^{Me}/PPh₃ ligand sphere in **6a** and IMes/PPh₃ in **1a** was most interestingly drawn out in studying the counterion dependence on catalyst reactivity (Table 5). Even at a relatively high and unoptimised catalyst loading of 5 mol%, larger and more weakly coordinating substrates **23**, **27**, and **28** perform relatively poorly when catalyst **6d**, bearing the OTf counter-ion, is used in the HIE reaction. Alternatively, the more strongly binding substrate, **29**, is relatively unaffected, and the order of reactivity generally reflects that previously observed when evaluating counter-ion effects with the IMes/PPh₃ combination [13]. Presumably, the smaller size of the IBn^{Me}/PPh₃ system suffers from competitive coordination of the triflate to the metal centre [32]. Most curiously, the catalyst series **6** is ineffective at labelling the weakly coordinating substrate, nitrobenzene **30**, whereas the flagship IMes/PPh₃ system **1a** labels to ~95% D under similar conditions [11]. This may be due to differences in available intermolecular (for example π - π) interactions of the substrate to the different catalyst systems upon binding. Nonetheless, such effects have the potential to be exploited favourably to induce directing group chemoselectivity in labelling multifunctional molecules.

Table 5. Evaluation of counter-ion effects in $\text{IBn}^{\text{Me}}/\text{PPh}_3$ complexes **6**.

Entry	Substrate	6a, X = PF ₆	6b, X = BF ₄	6c, X = SbF ₆	6d, X = OTf	6e, X = BAr ^F
1	23	96	96	96	79	97
2	27	91	87	93	29	97
3	28	98	87	93	43	99
4	29	82	89	90	85	87
5	30	5	4	5	4	16

3. Materials and Methods

See the Supplementary Information for details of all experimental and computational procedures, as well as all crystallographic data.

4. Conclusions

In summary, the first synthesis of the simple imidazolium-based natural product, Lepidiline A, **3·HCl**, has been reported, along with a range of other counter-ion derivatives. This has been followed by the development of novel HIE catalysts and the use of a silver-NHC transmetallation approach to HIE catalyst synthesis. Detailed and combined experimental/computational analysis of the resulting iridium complexes **6** and **7** has led to quantitative insight into the parameters responsible for observed differences in the resulting catalytic reactivity of **6a** versus the less substituted analogue, **7**, and existing flagship HIE catalyst, **1a**. Overall, dimethyl substitution on the backbone of the novel NHC was found to impart an electronic influence with a minimal impact on the steric environment. The reactivity differences between the catalysts studied are now being exploited in labelling regioselectivity studies, which will be reported in due course.

Supplementary Materials: All experimental procedures, computational calculations and X-ray structure data are available online at <http://www.mdpi.com/2073-4344/10/2/161/s1>: all experimental procedures along with corresponding compound characterisation; computational calculations for %V_{bur} in complexes **14–16** and C-H activation of acetophenone with catalysts **6a** and **7**; X-ray crystallographic parameters for compounds **3·HCl**, **3·HPF₆**, **12**, **14–16**, and **6a–6e**; and copies of all NMR spectra.

Author Contributions: Conceptualization, W.J.K. and T.T.; methodology, A.R.C. and M.R.; formal analysis, A.R.C., M.R. and A.R.K.; data curation, A.R.K. and D.M.L.; writing—original draft preparation, M.R. and D.M.L.; writing—review and editing, D.M.L. and W.J.K.; supervision, W.J.K.; funding acquisition, W.J.K. All authors have read and agreed to the published version of the manuscript.

Funding: We thank the Carnegie Trust (M.R.) for postgraduate studentship funding.

Acknowledgments: We acknowledge the EPSRC UK National Mass Spectrometry Facility at Swansea University for mass spectrometry analyses.

Conflicts of Interest: The authors declare no conflict of interest.

References and Note

1. Meyer, M.P. New Applications of Isotope Effects in the Determination of Organic Reaction Mechanisms. In *Advances in Physical Organic Chemistry*; Williams, I., Williams, N., Eds.; Elsevier: London, UK, 2012; Volume 46, pp. 57–114.
2. Isin, E.M.; Elmore, C.S.; Nilsson, G.N.; Thompson, R.A.; Weidolf, L. Use of radiolabeled compounds in drug metabolism and pharmacokinetic studies. *Chem. Res. Toxicol.* **2012**, *25*, 532–542. [[CrossRef](#)] [[PubMed](#)]
3. Penner, N.; Xu, L.; Prakash, C. Radiolabeled absorption, distribution, metabolism, and excretion studies in drug development: why, when and how? *Chem. Res. Toxicol.* **2012**, *25*, 513–531. [[CrossRef](#)] [[PubMed](#)]
4. Atzrodt, J.; Derdau, V.; Kerr, W.J.; Reid, M. Deuterium- and tritium-labelled compounds: Applications in the life sciences. *Angew. Chem. Int. Ed.* **2018**, *57*, 1758–1784. [[CrossRef](#)] [[PubMed](#)]
5. Schillerstrom, R. Heavy Drugs. *Drug Discov. Dev.* **2009**, *12*, 6–8.
6. Katsnelson, A. Heavy drugs draw heavy interest from pharma backers. *Nat. Med.* **2013**, *19*, 656. [[CrossRef](#)]
7. Atzrodt, J.; Derdau, V.; Kerr, W.J.; Reid, M. C-H functionalization for hydrogen isotope exchange. *Angew. Chem. Int. Ed.* **2018**, *57*, 3022–3047. [[CrossRef](#)]
8. Hesk, D. Highlights of C(sp²)-H hydrogen isotope exchange reactions. *J. Labelled Compd. Radiopharm.* **2019**. [[CrossRef](#)]
9. Valero, M.; Derdau, V. Highlights of aliphatic C(sp³)-H hydrogen isotope exchange reactions. *J. Labelled Compd. Radiopharm.* **2019**. [[CrossRef](#)]
10. Kerr, W.J.; Knox, G.J.; Paterson, L.C. Recent Advances in Iridium(I) Catalysis towards Directed Hydrogen Isotope Exchange. *J. Labelled Compd. Radiopharm.* **2019**. [[CrossRef](#)]
11. Brown, J.A.; Irvine, S.; Kennedy, A.R.; Kerr, W.J.; Andersson, S.; Nilsson, G.N. Highly Active Iridium(I) Complexes for Catalytic Hydrogen Isotope Exchange. *Chem. Commun.* **2008**, 1115–1117. [[CrossRef](#)]
12. Brown, J.A.; Cochrane, A.R.; Irvine, S.; Kerr, W.J.; Mondal, B.; Parkinson, J.A.; Paterson, L.C.; Reid, M.; Tuttle, T.; Andersson, S.; et al. The Synthesis of Highly Active Iridium(I) Complexes and Their Application in Catalytic Hydrogen Isotope Exchange. *Adv. Synth. Catal.* **2014**, *356*, 3551–3562. [[CrossRef](#)]
13. Kennedy, A.R.; Kerr, W.J.; Moir, R.; Reid, M. Anion Effects to Deliver Enhanced Iridium Catalysts for Hydrogen Isotope Exchange Processes. *Org. Biomol. Chem.* **2014**, *12*, 7927–7931. [[CrossRef](#)] [[PubMed](#)]
14. Kerr, W.J.; Mudd, R.J.; Paterson, L.C.; Brown, J.A. Iridium(I)-Catalyzed Regioselective C-H Activation and Hydrogen-Isotope Exchange of Non-Aromatic Unsaturated Functionality. *Chem. Eur. J.* **2014**, *20*, 14604–14607. [[CrossRef](#)] [[PubMed](#)]
15. Atzrodt, J.; Derdau, V.; Kerr, W.J.; Reid, M.; Rojahn, P.; Weck, R. Expanded Applicability of Iridium(I) NHC/Phosphine Catalysts in Hydrogen Isotope Exchange Processes with Pharmaceutically-Relevant Heterocycles. *Tetrahedron* **2015**, *71*, 1924–1929. [[CrossRef](#)]
16. Kerr, W.J.; Lindsay, D.M.; Reid, M.; Atzrodt, J.; Derdau, V.; Rojahn, P.; Weck, R. Iridium-Catalysed Ortho-H/D and -H/T Exchange under Basic Conditions: C–H Activation of Unprotected Tetrazoles. *Chem. Commun.* **2016**, *52*, 6669–6672. [[CrossRef](#)]
17. Kerr, W.J.; Mudd, R.J.; Owens, P.K.; Reid, M.; Brown, J.A.; Campos, S. Hydrogen Isotope Exchange with Highly Active Iridium(I) NHC/Phosphine Complexes: A Comparative Counterion Study. *J. Labelled Compd. Radiopharm.* **2016**, *59*, 601–603. [[CrossRef](#)]
18. Kerr, W.J.; Lindsay, D.M.; Owens, P.K.; Reid, M.; Tuttle, T.; Campos, S. Site-Selective Deuteration of N-Heterocycles via Iridium-Catalyzed Hydrogen Isotope Exchange. *ACS Catal.* **2017**, *7*, 7182–7186. [[CrossRef](#)]
19. Kerr, W.J.; Reid, M.; Tuttle, T. Iridium-Catalyzed C-H Activation and Deuteration of Primary Sulfonamides: An Experimental and Computational Study. *ACS Catal.* **2015**, *5*, 402–410. [[CrossRef](#)]
20. Kerr, W.J.; Reid, M.; Tuttle, T. Iridium-Catalyzed Formyl-Selective Deuteration of Aldehydes. *Angew. Chem. Int. Ed.* **2017**, *56*, 7808–7812. [[CrossRef](#)]
21. Cui, B.; Zheng, B.; He, K.; Zheng, Q. Imidazole Alkaloids from *Lepidium meyenii*. *J. Nat. Prod.* **2003**, *66*, 1101–1103. [[CrossRef](#)]
22. Curran, D.; Dada, O.; Müller-Bunz, H.; Rothmund, M.; Sánchez-Sanz, G.; Schobert, R.; Zhu, X.; Tacke, M. Synthesis and Cytotoxic Studies of Novel NHC*-Gold(I) Complexes Derived from Lepidiline A. *Molecules* **2018**, *23*, 2031. [[CrossRef](#)] [[PubMed](#)]
23. See the Supplementary Materials for further details.

24. Cochrane, A.R.; Irvine, S.; Kerr, W.J.; Reid, M.; Andersson, S.; Nilsson, G.N. Application of neutral iridium(I) N-heterocyclic carbene complexes in ortho-directed hydrogen isotope exchange. *J. Labelled Compd. Radiopharm.* **2013**, *46*, 451–454. [[CrossRef](#)]
25. Wang, H.M.J.; Lin, I.J.B. Facile Synthesis of Silver(I)–Carbene Complexes. Useful Carbene Transfer Agents. *Organometallics* **1998**, *17*, 972–975. [[CrossRef](#)]
26. Chang, Y.-H.; Fu, C.-F.; Liu, Y.-H.; Peng, S.-M.; Chen, J.-T.; Liu, S.-T. Synthesis, characterization and catalytic activity of saturated and unsaturated N-heterocyclic carbene iridium(I) complexes. *Dalton Trans.* **2009**, 861–867. [[CrossRef](#)] [[PubMed](#)]
27. Tolman, C.R. Steric effects of phosphorus ligands in organometallic chemistry and homogeneous catalysis. *Chem. Rev.* **1977**, *77*, 313–348. [[CrossRef](#)]
28. Mantilli, L.; Gérard, D.; Besnard, C.; Mazet, C. Structure-Activity Relationship in the Iridium-Catalyzed Isomerization of Primary Allylic Alcohols. *Eur. J. Inorg. Chem.* **2012**, *2012*, 3320–3330. [[CrossRef](#)]
29. Díez-González, S.; Nolan, S.P. Stereoelectronic parameters associated with N-heterocyclic carbene (NHC) ligands: A quest for understanding. *Coord. Chem. Rev.* **2007**, *251*, 874–883.
30. Nelson, D.J.; Truscott, B.J.; Slawin, A.M.Z.; Nolan, S.P. Synthesis and Reactivity of New Bis(N-heterocyclic carbene) Iridium(I) Complexes. *Inorg. Chem.* **2013**, *52*, 12674–12681. [[CrossRef](#)]
31. Torres, O.; Martín, M.; Sola, E. Labile N-Heterocyclic Carbene Complexes of Iridium. *Organometallics* **2009**, *28*, 863–870. [[CrossRef](#)]
32. Smidt, S.P.; Zimmermann, N.; Studer, M.; Pfaltz, A. Enantioselective Hydrogenation of Alkenes with Iridium–PHOX Catalysts: A Kinetic Study of Anion Effects. *Chem. Eur. J.* **2004**, *10*, 4685–4693. [[CrossRef](#)]



© 2020 by the authors. Licensee MDPI, Basel, Switzerland. This article is an open access article distributed under the terms and conditions of the Creative Commons Attribution (CC BY) license (<http://creativecommons.org/licenses/by/4.0/>).